Supplement of

Cross-phase partitioning of sulfur-nitrogen ratios and aerosol mixing-state evolution based on single-particle observations

Yuan Dai et al.

Correspondence to: Xinlei Ge (xinlei@seu.edu.cn), Junfeng Wang (wangjunfeng@nuist.edu.cn)

Table S1. Summary of descriptions of particle types during the whole campaign.

Category	Particle types	Fraction in total		Dominant ions in mass spectrum
		Winter	Summer	
BC	BC-pure	0.5%	2.0%	$12[C]^{+}\sim120[C_{10}]^{+}$, $39[K]^{+}$ $-24[C_2]^{-}\sim-108[C_9]^{-}$
	BC-S	4.6%	7.7%	$12[C]^{+}\sim60[C_5]^{+}$, $39[K]^{+}$ $-24[C_2]^{-}\sim-48[C_4]^{-}$, $-97[HSO_4]^{-}$
	BC-N	29.3%	15.2%	$12[C]^{+}\sim60[C_5]^{+}$, $39[K]^{+}$ $-24[C_2]^{-}\sim-48[C_4]^{-}$, $-46[NO_2]^{-}$, $-62[NO_3]^{-}$
	BC-SN	3.0%	0.9%	$12[C]^{+}\sim60[C_5]^{+}$, $39[K]^{+}$ $-24[C_2]^{-}\sim-48[C_4]^{-}$, $-46[NO_2]^{-}$, $-62[NO_3]^{-}$, $-97[HSO_4]^{-}$
	BC-CN	5.9%	10.5%	$12[C]^{+}\sim60[C_5]^{+}$, $39[K]^{+}$ $-24[C_2]^{-}\sim-48[C_4]^{-}$, $-26[CN]^{-}$, $-42[CNO]^{-}$, $-46[NO_2]^{-}$, $-62[NO_3]^{-}$, $-97[HSO_4]^{-}$
BCOC	BCOC-S	4.6%	8.4%	$12[C]^{+}\sim60[C_5]^{+}$, $37[C_3H^{+}]$, $39[K]^{+}/39[C_3H_3]^{+}$, $43[C_2H_3O]^{+}$,$51[C_4H_3]^{+}$ $-24[C_2]^{-}\sim-48[C_4]^{-}$, $-97[HSO_4]^{-}$
	BCOC-N	6.4%	5.9%	$12[C]^{+}\sim60[C_5]^{+}$,$37[C_3H^{+}]$,$39[K]^{+}/39[C_3H_3]^{+}$,$43[C_2H_3O]^{+}$,$51[C_4H_3]^{+}$ $-24[C_2]^{-}\sim-48[C_4]^{-}$, $-46[NO_2]^{-}$, $-62[NO_3]^{-}$
	BCOC-SN	2.1%	1.3%	$12[C]^{+}\sim60[C_5]^{+}$,$37[C_3H^{+}]$,$39[K]^{+}/39[C_3H_3]^{+}$,$43[C_2H_3O]^{+}$,$51[C_4H_3]^{+}$ $-24[C_2]^{-}\sim-48[C_4]^{-}$, $-46[NO_2]^{-}$, $-62[NO_3]^{-}$, $-97[HSO_4]^{-}$
	BCOC-CN	2.7%	6.2%	$12[C]^{+}\sim60[C_5]^{+}$,$37[C_3H^{+}]$,$39[K]^{+}/39[C_3H_3]^{+}$,$43[C_2H_3O]^{+}$,$51[C_4H_3]^{+}$ $-24[C_2]^{-}\sim-48[C_4]^{-}$, $-26[CN]^{-}$, $-42[CNO]^{-}$, $-46[NO_2]^{-}$, $-62[NO_3]^{-}$, $-97[HSO_4]^{-}$
BF (BCfree)	BF-S	3.5%	4.0%	$18[NH_4]^{+}$, $23[Na]^{+}$, $39[K]^{+}$, $40[Ca]^{+}$ $-97[HSO_4]^{-}$
	BF-N	17.8%	13.7%	$18[NH_4]^{+}$, $23[Na]^{+}$, $39[K]^{+}$, $40[Ca]^{+}$ $-46[NO_2]^{-}$, $-62[NO_3]^{-}$
	BF-SN	2.4%	0.6%	$18[NH_4]^{+}$, $23[Na]^{+}$, $39[K]^{+}$, $40[Ca]^{+}$ $-46[NO_2]^{-}$, $-62[NO_3]^{-}$, $-97[HSO_4]^{-}$
	BF-CN	2.9%	4.6%	$18[NH_4]^{+}$, $23[Na]^{+}$, $39[K]^{+}$, $40[Ca]^{+}$ $-26[CN]^{-}$, $-42[CNO]^{-}$, $-46[NO_2]^{-}$, $-62[NO_3]^{-}$, $-97[HSO_4]^{-}$
BFOC	BFOC-S	3.8%	5.2%	$37[C_3H^{+}]$, $39[K]^{+}/39[C_3H_3]^{+}$, $43[C_2H_3O]^{+}$, $51[C_4H_3]^{+}$ $-97[HSO_4]^{-}$
	BFOC-N	5.6%	5.2%	$37[C_3H^{+}]$, $39[K]^{+}/39[C_3H_3]^{+}$, $43[C_2H_3O]^{+}$, $51[C_4H_3]^{+}$ $-46[NO_2]^{-}$, $-62[NO_3]^{-}$
	BFOC-SN	1.8%	1.0%	$37[C_3H^{+}]$, $39[K]^{+}/39[C_3H_3]^{+}$, $43[C_2H_3O]^{+}$, $51[C_4H_3]^{+}$ $-46[NO_2]^{-}$, $-62[NO_3]^{-}$, $-97[HSO_4]^{-}$
	BFOC-CN	1.6%	2.6%	$37[C_3H^{+}]$, $39[K]^{+}/39[C_3H_3]^{+}$, $43[C_2H_3O]^{+}$, $51[C_4H_3]^{+}$ $-26[CN]^{-}$, $-42[CNO]^{-}$, $-46[NO_2]^{-}$, $-62[NO_3]^{-}$, $-97[HSO_4]^{-}$
OTHER	BC-other	0.8%	2.1%	Remaining BC containing particles that do not belong to the BC containing types listed above
	BF-other	0.8%	2.6%	Remaining BC-free particles that do not belong to the BC-free types listed above

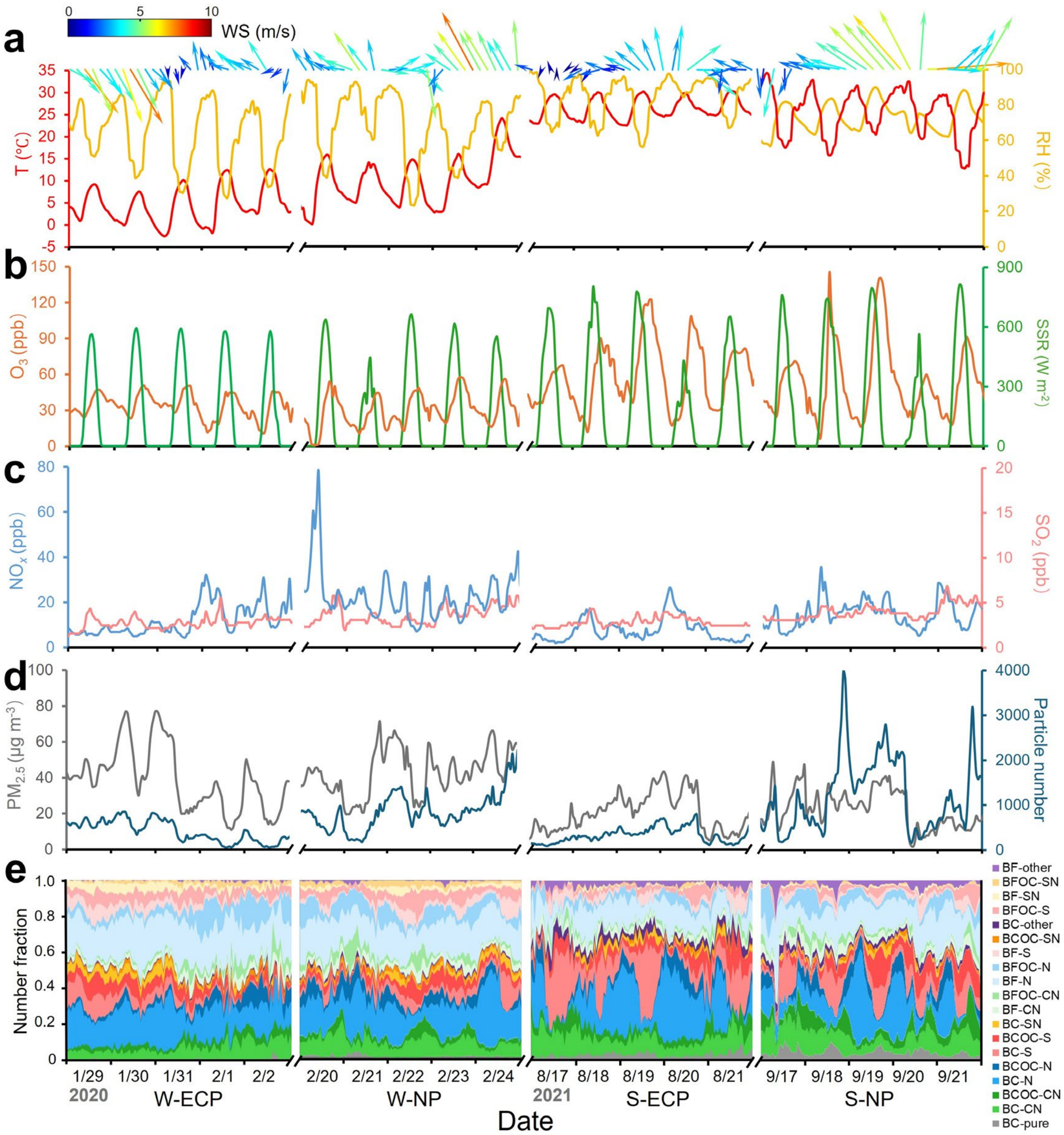

Figure S1. Time series of meteorological variables and chemical species measured in Yangzhou during the winter emission control period (W-ECP), winter normal period (W-NP), summer emission control period (S-ECP), and summer normal period (S-NP). (a) Wind speed (WS, m s^{-1}), wind direction (WD, °), air temperature (T, °C), and relative humidity (RH, %). (b) Ozone (O_3, ppb), and surface sun radiation (W m^{-2}). (c) Gaseous pollutants NO_x and SO_2 (ppb). (d) $PM_{2.5}$ mass concentration (μg m^{-3}) and total particle number concentration. (e) Number fractions of different single-particle classes.

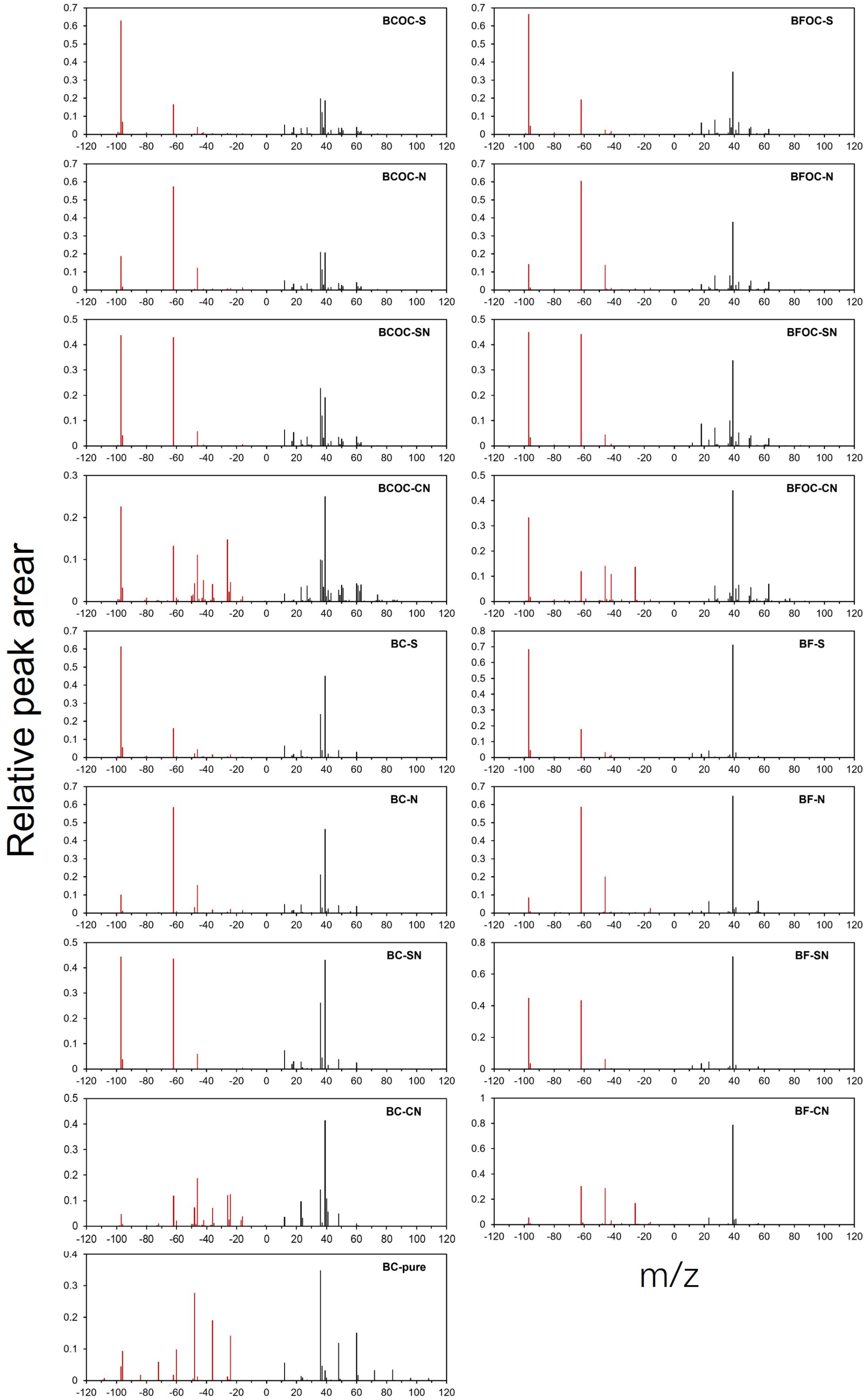

Figure S2. Mass spectrum of identified single particle types.

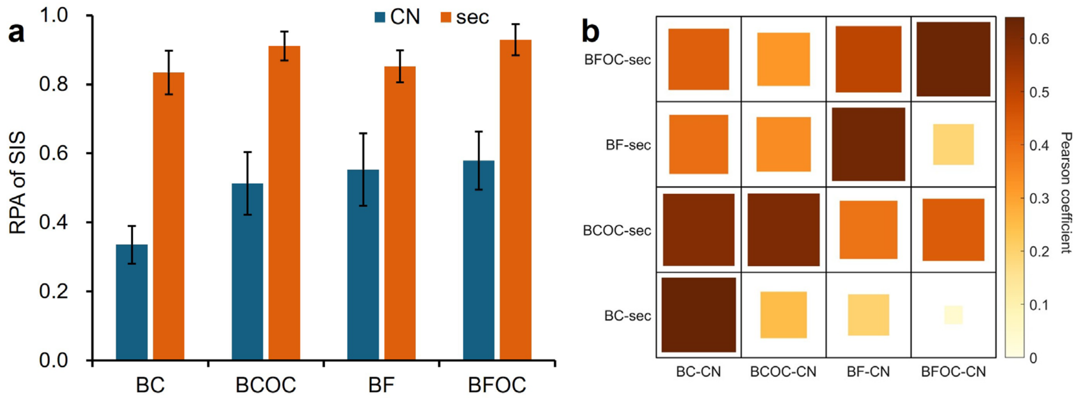

Figure S3. Evidence supporting the operational definition of fresh-like (-CN) and aged-like (-sec) subclasses across principal particle groups. (a) Fractional secondary inorganic species (SIS) signal, calculated as the sum of the normalized peak areas of −97[HSO_4^-], −96[SO_4^{2-}], −62[NO_3^-], and −46[NO_2^-]. (b) Pearson correlation matrix between hourly number concentrations of fresh-like (columns) and aged-like (rows) subclasses.

Table S2. Summary of datasets and variables used in this study, including emissions, meteorological fields, and sulfur-to-nitrogen ratio indicators.

Dataset	Variable	Content	Unit	Spatial resolution	Temporal resolution	Data source
Emission	$PM_{2.5}$	Particulate matter ≤ 2.5 μm	μg m^{-3}	in situ	hourly	On-line measurements
	PM_{10}	Particulate matter ≤ 10 μm	μg m^{-3}			
	NO_x	Nitrogen oxide	ppb			
	SO_2	Sulfur dioxide	ppb			
	CO	Carbon monoxide	ppm			
	O_3	Ozone	ppb			
Meteorology	T2m	2m air temperature	K	0.1° × 0.1°	hourly	ERA5-Land*
	T10m	2m air temperature	K			
	DP2m	Dew point temperature	K			
	U2m	2-meter eastward wind	m s^{-1}			
	V2m	2-meter northward wind	m s^{-1}			
	TPREC	Total precipitation	m			
	SSR	Surface net solar radiation	J m^{-2}			
	RH	Relative humidity	%	0.25° × 0.25°		GEOS-CF**
	SLP	Sea level pressure	Pa			
	BLH	Planetary boundary layer height	m			
SNRs	gSNR	The molar ratios of SO_2 to NO_x	—	in situ	hourly	On-line measurements
	pSNR	The peak area ratios of sulfate to nitrate	—			SPA-MS
	nSNR	The number ratios of sulfate to nitrate	—			

*https://developers.google.com/earth-engine/datasets/catalog/ECMWF_ERA5_LAND_HOURLY

**https://developers.google.com/earth-engine/datasets/catalog/NASA_GEOS-CF_v1_rpl_tavg1hr

Table S3. Values of hygroscopic parameter κ and dry bulk density ρ.

Species	κ	ρ (g cm^{-3})	Reference
$(NH_4)_2SO_4$	0.53	1.76	(Petters and Kreidenweis, 2007)
NH_4NO_3	0.58	1.72	(Petters and Kreidenweis, 2007)
KCl	0.99	1.99	(Carrico et al., 2010)
OC	0.03	1.00	(Saxena and Hildemann, 1996)
BC	0	1.80	(Bond and Bergstrom, 2006)

Densities are taken from Lide (2005)(Lide, 1995).

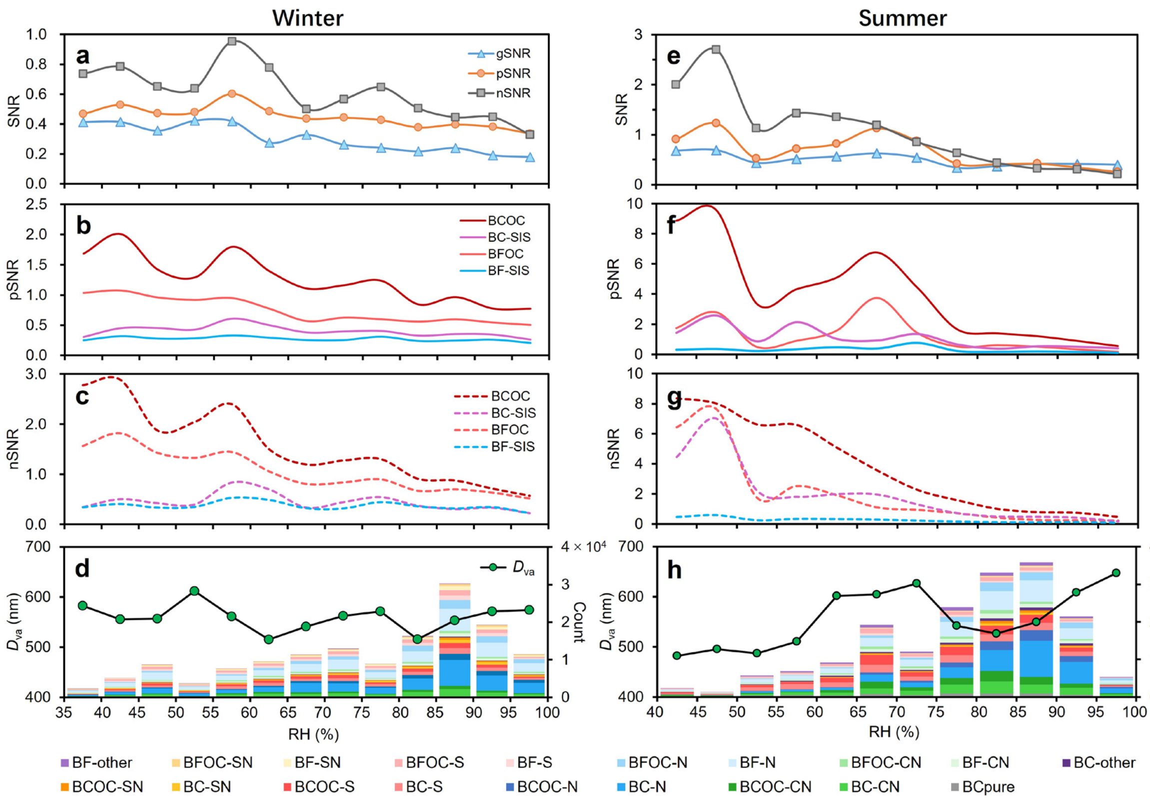

Figure S4. Variations in sulfur-to-nitrogen ratios (SNR) with relative humidity (RH) for different aerosol particle types during winter (a-d) and summer (e-h). (a, e) Trends of gas-phase (gSNR), particle-phase (pSNR), and number-based (nSNR) ratios across the RH gradient; (b, f) pSNR variations with RH for aged-like BC-containing and BC-free particle types; (c, g) nSNR trends across different aged-like particle types as a function of RH; (d, h) Corresponding changes in vacuum aerodynamic diameter (D_{va}, green line, left axis) and number concentration (bars, right axis) of individual particle types with RH.

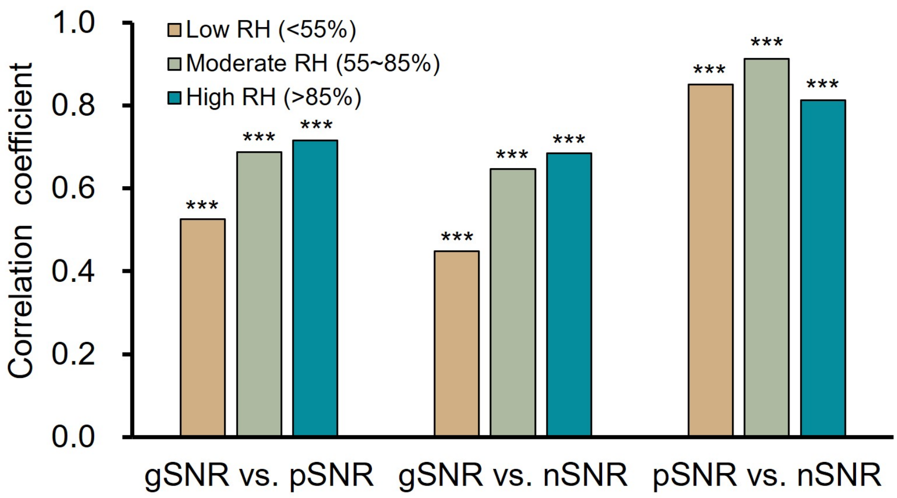

Figure S5. Correlation coefficients among gas-phase, particle-phase, and number-based sulfur-to-nitrogen ratios (gSNR, pSNR, nSNR) under different relative humidity (RH) regimes. Asterisks indicate statistical significance (*** $p<0.001$, Pearson correlation).

Table S4. Evaluation of the SSA-XGBoost regression model

Species	pSNR		nSNR	
	RMSE	R^2	RMSE	R^2
BCOC-sec	2.23	0.71	2.84	0.74
BC-sec	0.74	0.91	2.21	0.94
BFOC-sec	0.80	0.86	1.33	0.77
BF-sec	0.54	0.77	0.52	0.82
ALL	0.72	0.74	2.48	0.85

[a]RMSE (Root mean square error) is the square root of the expected squared difference between the predicted and observed values.
[b]R^2 is the correlation between the observed and SSA-XGBoost predicted SNRs.

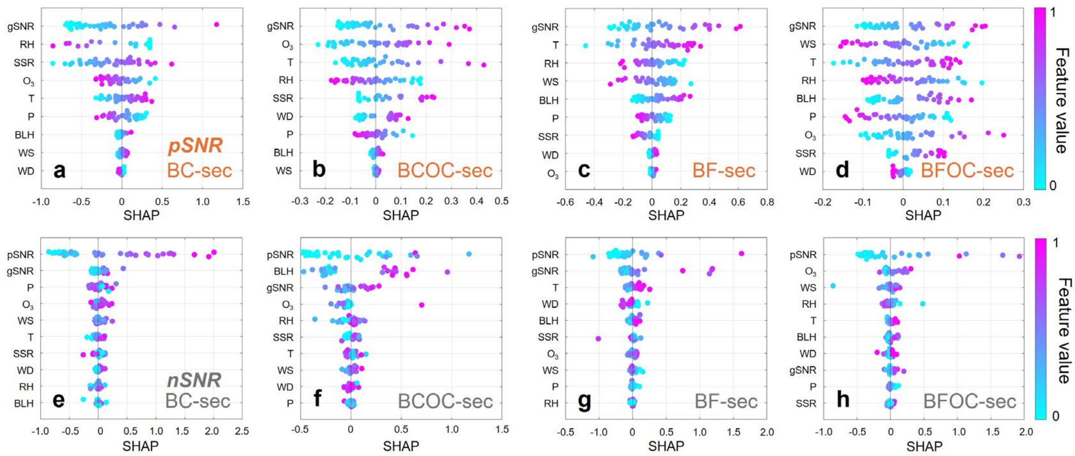

Figure S6. SHAP summary plots show the relative importance of predictors for particle-phase (pSNR; a-d) and number-based (nSNR; e-h) sulfur-to-nitrogen ratios.

References:

Bond, T.C., Bergstrom, R.W., 2006. Light absorption by carbonaceous particles: An investigative review. Aerosol Sci. Technol. 40, 27–67. https://doi.org/10.1080/02786820500421521

Carrico, C.M., Petters, M.D., Kreidenweis, S.M., Sullivan, A.P., McMeeking, G.R., Levin, E.J.T., Engling, G., Malm, W.C., Collett, J.L.J., 2010. Water uptake and chemical composition of fresh aerosols generated in open burning of biomass. Atmospheric Chem. Phys. 10, 5165–5178. https://doi.org/10.5194/acp-10-5165-2010

Lide, D.R., 1995. CRC handbook of chemistry and physics: A ready-reference book of chemical and physical data. CRC Press.

Petters, M.D., Kreidenweis, S.M., 2007. A single parameter representation of hygroscopic growth and cloud condensation nucleus activity. Atmospheric Chem. Phys. 7, 1961–1971. https://doi.org/10.5194/acp-7-1961-2007

Saxena, P., Hildemann, L.M., 1996. Water-soluble organics in atmospheric particles: A critical review of the literature and application of thermodynamics to identify candidate compounds. J. Atmospheric Chem. 24, 57–109. https://doi.org/10.1007/BF00053823